Lawrence Berkeley National Laboratory
Recent Work

Title
FIELD ION MICROSCOPIC OBSERVATIONS OF DISLOCATION STRUCTURES AT GRAIN BOUNDARIES

Permalink
https://escholarship.org/uc/item/6g776214

Author
Ranganathan, S.

Publication Date
1966-05-01

University of California

Ernest O. Lawrence Radiation Laboratory

FIELD ION MICROSCOPIC OBSERVATIONS OF DISLOCATION
STRUCTURES AT GRAIN BOUNDARIES

DISCLAIMER

UNIVERSITY OF CALIFORNIA

Lawrence Radiation Laboratory
Berkeley, California

FIELD ION MICROSCOPIC OBSERVATIONS OF DISLOCATION
STRUCTURES AT GRAIN BOUNDARIES

S. Ranganathan

May 1966

FIELD ION MICROSCOPIC OBSERVATIONS OF DISLOCATION
STRUCTURES AT GRAIN BOUNDARIES

S. Ranganathan[*]

Inorganic Materials Research Division, Lawrence Radiation Laboratory,
Department of Metallurgy, College of Engineering,
University of California, Berkeley, California

May 1966

ABSTRACT

The nature of dislocation contrast in field ion micrographs is

examined and it is shown that spirals should be observed in most

orientations. This analysis is extended to the spiral structures

observed at boundaries and evidence for dislocations at a low angle

boundary, a noncoherent twin, and a random boundary is presented in

the context of lattice coincidence.

[*] This work was performed at the Department of Metallurgy, Cambridge,
England.

I. INTRODUCTION

The field ion microscope has been used by a number of investigators
for the elucidation of the atomic configuration at high angle grain
boundaries. A model based on the coincidence site lattice was developed
as a result of a study by Brandon, Ralph, Ranganathan, and Wald.[1] This
model postulated that special boundaries should show good fit over large
regions and give rise to a stepped structure when the plane of the boundary
deviated from densely packed coincidence site lattice planes. For mis-
orientations away from those characterizing partial lattice coincidence,
a sub-boundary has to be added to the special boundary. It can be seen
that the model demands a structure based on dislocations for most orien-
tations. The field ion micrographs have demonstrated the narrow width
of high angle boundaries and also the presence of ledges only a few
Angstroms in height.[1] The evidence for the dislocation part of the
model rested on dark bands observed at random boundaries. These dark
bands were similar to those that had been observed earlier at low angle
boundaries by Brandon and his co-workers[2] and had been attributed to the
effect of preferential evaporation occurring as a result of the strain
field of the dislocations. Further observations[3] have shown that this
effect does not occur at all low-angle boundaries. It appears that
electronic effects can play an important part in the image contrast at
grain boundaries and can lead to the appearance of streaks and dark
bands. This has been discussed by Ranganathan et al.[4] The contrast from
individual dislocation is examined in this paper and is correlated with
the observation of dislocation structures at grain boundaries. These
results were first presented by the author at the 11th Field Emission
Symposium in Cambridge (1964) and the 12th Field Emission Symposium in
State College (1965).

2. CONTRAST FROM DISLOCATIONS

The dislocation observed in a field ion specimen is emerging at the surface of a nearly hemispherical crystal. The imaging field imposes a stress (largely hydrostatic) on the specimen. Finally the surface has been prepared by field evaporation. All three factors have to be taken into account in the interpretation of dislocation contrast. However a useful starting point is to consider the microtopography of the surface where the dislocation intersects it and to establish the Burgers vector $\bar{b}$ of the dislocation. The direction $\bar{n}$ of the dislocation line can be easily determined by the use of field evaporation.

Drechsler[5] has analyzed the configurations resulting from the emergence of screw dislocations on the surface of a bcc metal crystal and showed that spirals are to be expected. At that period, hydrogen ion microscopy at room temperature was used with consequent poor resolution and spiral structures were shown to result after heating the tip *in situ*. In 1958, Müller[6] convincingly demonstrated that these are only pseudo-spirals caused by a bunching of planes brought about by surface migration. Such spirals became resolved as closed net plane edges when imaged at a voltage slightly higher than the best image voltage. Also it appears that Drechsler[5] considered a dislocation with a Burgers vector of a [110] in bcc lattice. In this article we consider only the characteristic dislocations in bcc and fcc lattices.

2.1. Determination of the Burgers Vector

The planes [indices {hkl} and plane normal $\bar{g}$] appearing in a field-ion micrograph fall into two categories. In close-packed planes atomic resolution is obtained only around the edge. Their general appearance

is a series of concentric rings (e.g., {011}, {001}, {112}, {013} in tungsten; {111}, {001}, {113}, {011} in iridium). In loose-packed planes individual atoms are seen over the entire plane but in general the number of rings corresponding to a particular set of indices (hkl) is small. The contrast effect from dislocations also differs to some extent on these two categories of planes.

The contrast for the case of a dislocation running at angle to the plane, i.e., $\bar{n} \cdot \bar{g} \neq 0$ is considered here. (The case where the dislocation occupies the extent of a single plane and is fully within the field of view should be rare and does not concern us further.) Two situations arise.

(a) $\bar{n} \cdot \bar{g} \neq 0$, $\bar{g} \cdot \bar{b} = 0$. In this event the Burgers vector lies in the plane and the displacement is therefore confined to the plane. The close-packed planes will remain as concentric rings and the dislocation may escape observation. Examples have been given by Ryan and Suiter[7] and Ranganathan.[8] The dislocation is effectively invisible and the analogy with other methods of diffraction is suggestive. When the dislocation intersects a loose-packed plane and the Burgers vector lies in that plane, then the Burgers vector can, however, be determined by the construction of a Burgers circuit -- a tribute to the directness of the technique.

(b) $\bar{n} \cdot \bar{g} \neq 0$, $\bar{g} \cdot \bar{b} \neq 0$. In this case the net plane rings do not close on themselves but form a continuous spiral. The spiral is due to the component of the Burgers vector normal to the plane. This vertical component is always equal to an integral number of interplanar spacing. If the vertical component is equal to a single interplanar spacing (the usual case for close-packed planes) a simple spiral will arise. A set of interleaved helicoids will result if the vertical

component is equal to a number of interplanar spacings. Table I gives
the type of spirals expected on close-packed planes in the bcc lattice
when dislocations with characteristic Burgers vectors intersect the
surface. The nature of the spiral allows the vertical component of the
Burgers vector to be determined. Further characterization of the Burgers
vector can be done only in cases where the direction of the dislocation
line is such that it intersects different crystal planes on field evapora-
tion. For this to occur the dislocation line must be inclined to the
axis of the wire.

An example here illustrates the foregoing considerations. A dis-
location with $a/2[111]$ will give rise to a single spiral on $(21\bar{1})$, a
single spiral on (110), and a two-leaved spiral on (121). A dislocation
with $a/2[\bar{1}11]$ will give rise to a single spiral on $(21\bar{1})$, will be
invisible on (011), and again give rise to a single spiral on (121).
Thus the different behaviors can be used for obtaining information on
the Burgers vectors. The procedure is analogous to tilting experiments
in electron microscopy.

A second possibility for the determination of Burgers vectors exists
when a low angle boundary intersects different planes. The boundary is
composed of a set of dislocations with a given Burgers vector and hence
the topography of various planes should be informative. Complications
can arise however when the boundary is composed of more than one set
of dislocations.

When there is more than one dislocation emerging at the surface,
the crystal consists of a number of interleaved "expanded Riemann surfaces".[9]
In a simple case where two dislocations of opposite character emerge, a
horseshoe-shaped net plane results and has been noted by Müller.[10]

TABLE I. Expectancy and nature of spirals based
on g · b ≠ 0 criterion.

g \ b	a/2[111]	a/2[Ī11]	a/2[1Ī1]	a/2[11Ī]
110	Single	No spiral	No spiral	Single
01Ī	No spiral	No spiral	Single	Single
10Ī	No spiral	Single	No spiral	Single
101	Single	No spiral	Single	No spiral
011	Single	Single	No spiral	No spiral
1Ż1	No spiral	Single	Two leaved	Single
11Ż	No spiral	Single	Single	Two leaved
21Ī	Single	Single	No spiral	Two leaved
211	Two leaved	No spiral	Single	Single
112	Two leaved	Single	Single	No spiral
121	Two leaved	Single	No spiral	Single
020	Single	Single	Single	Single
200	Single	Single	Single	Single

Spirals are a general contrast effect arising from dislocation. Their nature gives information concerning the Burgers vector. From a knowledge of b̄, and the direction of the dislocation, the character of the dislocation in terms of edge and screw components can be deduced.

3. OBSERVATIONS

3.1. Dislocation Structure at Low Angle Boundaries

Several instances where the dislocation arrays at a low angle bound-
ary could be resolved were recorded. If there are to be five dislocations
in the field of view, the dislocation will be about 60 Å apart. This
distance of separation will correspond in the case of a simple tilt bound-
ary to a misorientation of $3°$. The grain boundary in iridium shown in
Fig. 1 has a misorientation of 2° around [111]. The plane of the boundary
was inclined to the axis of the wire and the boundary intersected the
surface at a different place on field evaporation. The asymmetry of the
tip made an accurate determination of the plane of the boundary impossible.
The streaks occur on (01$\bar{1}$) planes in fcc metals. The intersection of the
boundary is parallel to the streaks showing that their poles occur in the
same zone. This fact and the movement of the boundary intersection
pointed to (120) as the boundary plane. Hence the boundary has twist
character and must have screw dislocations making up the array.

The dislocation structure in Fig. 1 has the appearance of a "classical"
screw dislocation. If the boundary plane is (111) and if the axis of mis-
orientation is [111], the model for the boundary consists of a hexagonal
grid of dislocations having Burgers vectors a/2[1$\bar{1}$0], a/2[$\bar{1}$01], and
a/2[01$\bar{1}$]. When the orientation of the boundary plane is changed, e.g.,
to (120), there is only a change in the mesh shape and the pattern
becomes such that its projection along the [111] on a (111) plane pro-
duces the same hexagonal net. The dislocation seen at the boundary must
form part of such a grid. However the Burgers vectors of the dislocation
must be of the type a/2[110] or a/2[101] or a/2[011]. The reason for
this is clear from the considerations offered in Sec. 2.1. a/2[1$\bar{1}$0],

a/2[Ī01], and a/2[01Ī] all lie on the (111) plane and hence will not give rise to a spiral based on (111) planes. The dislocation is thus probably a stranger dislocation in the network.

Interlocked and interleaved spirals have been observed at low angle boundaries in tungsten and molybdenum. They are not easily analyzed into the component dislocations.

3.2. Dislocation Structures at Twin Boundaries

Twinning is a mode of deformation and is especially favored at low temperatures and high strain rates in the case of bcc metals (Hall).[11] In three instances deformation twinning of the tips was observed. Figures 2 and 3 were obtained before and after the twinning transformation. The poles [110] and [112] remain in the same position as a twin can be related by a 70.5° rotation around [110] and a 180° rotation around [112]. It can also be noted that the zone decoration line has rotated through 70°. The tip was originally hemispherical and has become ellipsoidal as a result of twinning. There is considerable stress relief and the tilt in the surface could have led to the observed streaking.

In another case twinning occurred as the voltage was raised to the value necessary for imaging. The boundary region appeared as a chasm at first and gradually this closed up. A cavity can still be seen in Fig. 4. The twin relationship is obvious. The spiral effect implies that a dis- location structure has been added to the boundary. The spiral is similar to the one observed at the low angle boundary in iridium. The continuity of the spiral is interrupted at the ninth plane where a second dislocation might be intersecting the surface. The twin has a noncoherent interface and the plane of the boundary is very near {112}$_A$ and {110}$_B$. Both are close-packed planes in the bcc lattice, and this explains the excellent

atomic matching across the boundary. The dislocation observed near the central (110) pole will explain the slight deviation in the plane of the boundary from the close-packed planes. In this case the orientation relationship is exact and hence there is no superposed small angle boundary.

With field evaporation, the spiral remained in the same place thus showing that the dislocation was running in the (110) direction. Similar spirals arising through evaporation have been observed on a macroscopic scale by Votava and Berghezan.[12] They ascribed the spirals to twinning dislocations. It is difficult to see how a single twinning dislocation can give rise to a simple spiral. Obviously a number of partial dislocations together can give rise to a spiral. The suggestion of Ryan and Suiter[13] that these structures result from slip dislocation adsorbed at the boundary is attractive. However, even in this case, because the crystals are rotated with respect to each other, the continuation of the atomic planes across the boundary is surprising.

3.3. Dislocation Structures at Random Boundaries

Figure 5 shows a grain boundary in molybdenum. The misorientation is around the [110] axis and is $30°$. The relationship is $3°$ away from [110] - $27°$ which represents a special boundary with a density of coincidence of 1 in 19. One can then consider the boundary to be made up of this special boundary and a $3°$ small angle boundary. The spiral effect seen in the (110) planes has its origin in the latter boundary. The boundary plane is a few degrees of $(1\bar{1}0)_B$ and $(3\bar{3}2)_A$ and is near a densely packed coincidence site lattice plane of [331] type in both crystals. This accounts for the atomic matching across the boundary.

In the iridium example the dislocation formed of a low angle boundary:
in the case of tungsten, it accounted for the deviation of the grain bound-
ary from a close-packed plane. Now in molybdenum a similar spiral forms
part of the small angle boundary superposed on a special boundary.

Figure 6 shows a tricrystal in iridium. The boundary B-C corresponds
to a $6°$ misorientation around [111]. The boundary appears very nearly as
a streak. Most (111) planes are seen to join smoothly across the boundary.
Boundary A-B is a high angle boundary with a misorientation of $52°$ around
[111]. The nearest coincidence site lattice is $5°$ away. The boundary is
quite narrow and showed extremely good fit over nearly a hundred layers.
The good fit observed at the boundary A-B merits some discussion. The
orientation relationship for this boundary is $5°$ away from [111] - $47°$
which is the relationship for a coincidence site lattice of $\Sigma = 19$. This
lattice is illustrated in Fig. 7. It can be seen that the density of
coincidence is so low in this case that an associated $5°$ sub-boundary will
take out almost all lattice coincidence.

Figure 8 shows a [110] - $28°$ boundary in tungsten. There appears to
be a dark band associated with the boundary. On field evaporation this
band became less prominent as the intersection of the boundary moved
inwards due to the inclination of the plane of the boundary to the axes
of the tip. One can see a series of interlocked spirals. In some
regions the continuation of the (110) planes across the boundary can
be followed through a number of planes.

4. DISCUSSIONS

Since the original paper by Brandon et al.[1] was written, a large number of field-ion microscopic observations of high angle grain boundaries in a variety of metals has been made. One can distinguish three types of structures. In one kind the dominant, close-packed planes continue undisturbed across the boundary. Such structures have been observed in coherent and noncoherent twins.[14,15] Ryan and Suiter[13] have shown such a structure for a misorientation of $32°$ around [110]. As discussed in Sec. II, these boundaries can contain dislocations which have their Burgers vector parallel to the undisturbed planes. In the second kind, spiral structures which can generally be associated with dislocations have been observed. Ryan and Suiter[13] have shown spirals in tungsten and molybdenum as well as a spiral at a low angle boundary in iridium. It appears that one can expect such spirals in boundaries in both bcc and fcc metals. The third kind is the usual case and in this the boundaries show a greater degree of disturbance (Figs. 6 and 8). All three observations are in conformity with the idea of a transition lattice structure at the boundary where the change from one lattice to another occurs rapidly (in one or two atom layers). Moreover regions showing varying degrees of fit have been observed at these boundaries, and this seems to be in agreement with Mott's model. The coincidence site lattice model of Brandon et al.[1] attempts to characterise the region in precise crystallographic terms (Brandon[16] has recently extended the theoretical part of the model in a rigorous way). Section III presents some evidence that the regions of fit and the dislocation structure observed at boundaries can be interpreted with respect to lattice coincidence. A closer linkup must await a better understanding of the topography of a surface intersected by dislocations and grain boundaries.

UCRL-17331

ACKNOWLEDGMENTS

REFERENCES

1. D. G. Brandon, B. Ralph, S. Ranganathan, and M. Wald, Acta Met. 12, 813 (1964).

2. D. G. Brandon, M. Wald, M. J. Southon, and B. Ralph, J. Phys. Soc. Japan 18, 324 (1963).

3. S. Ranganathan and A. H. Cottrell, Electron Microscopy 64, Third European Regional Conference on Electron Microscopy, Prague, 1964, p. 163.

4. S. Ranganathan, K. M. Bowkett, J. Hren, and B. Ralph, Phil. Mag. 12, 841 (1965).

5. M. Drechsler, Z. Physik. Chem. 6, 272 (1956).

6. E. W. Müller, Acta Met. 6, 620 (1958).

7. H. F. Ryan and J. Suiter, J. Less Common Metals 9, 258 (1965).

8. S. Ranganathan, J. Less Common Metals 10, 368 (1966).

9. F. C. Frank, Advan. Phys. 1, 91 (1952).

10. E. W. Müller, J. Appl. Phys. 30, 1843 (1959).

11. E. O. Hall, Twinning (Butterworths Scientific Publications, London 1954).

12. E. Votava and A. Berghezan, Acta Met. 7, 392 (1959).

13. H. F. Ryan and J. Suiter, Acta Met. 14, 847 (1966).

14. E. W. Müller and O. Nishikawa, Technical Report AFML-TR-65-201, August 1965.

15. J. Hren, Acta Met. 13, 479 (1965).

16. D. G. Brandon (private communication).

FIGURE CAPTIONS

Fig. 1   A low angle boundary in iridium. Note the spiral. The
          angle of misorientation is 2° and the axis of misorientation
          [111].

Fig. 2   Tungsten surface before deformation twinning.

Fig. 3   Same surface as in Fig. 2 after twinning.

Fig. 4   Spiral structure at a twin interface in tungsten.

Fig. 5   A random boundary in molybdenum. The spiral arises from a 3°
          boundary added to a special boundary.

Fig. 6   Tricrystal in iridium.

Fig. 7   Coincidence site lattice for a density of 1 in 19. The high
          angle boundary in Fig. 6 is related to this.

Fig. 8   A random boundary in tungsten with a small deviation from
          lattice coincidence.
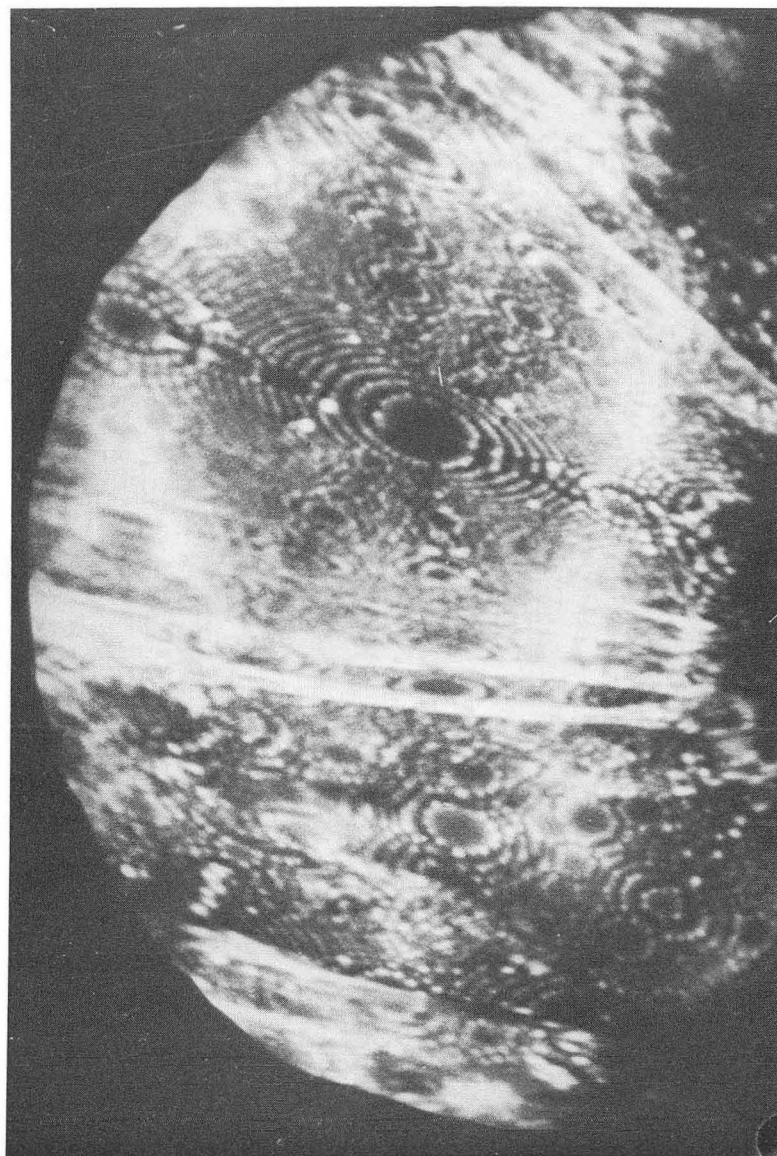
ZN-5393

Fig. 1

ZN-5454

Fig. 2

-16-
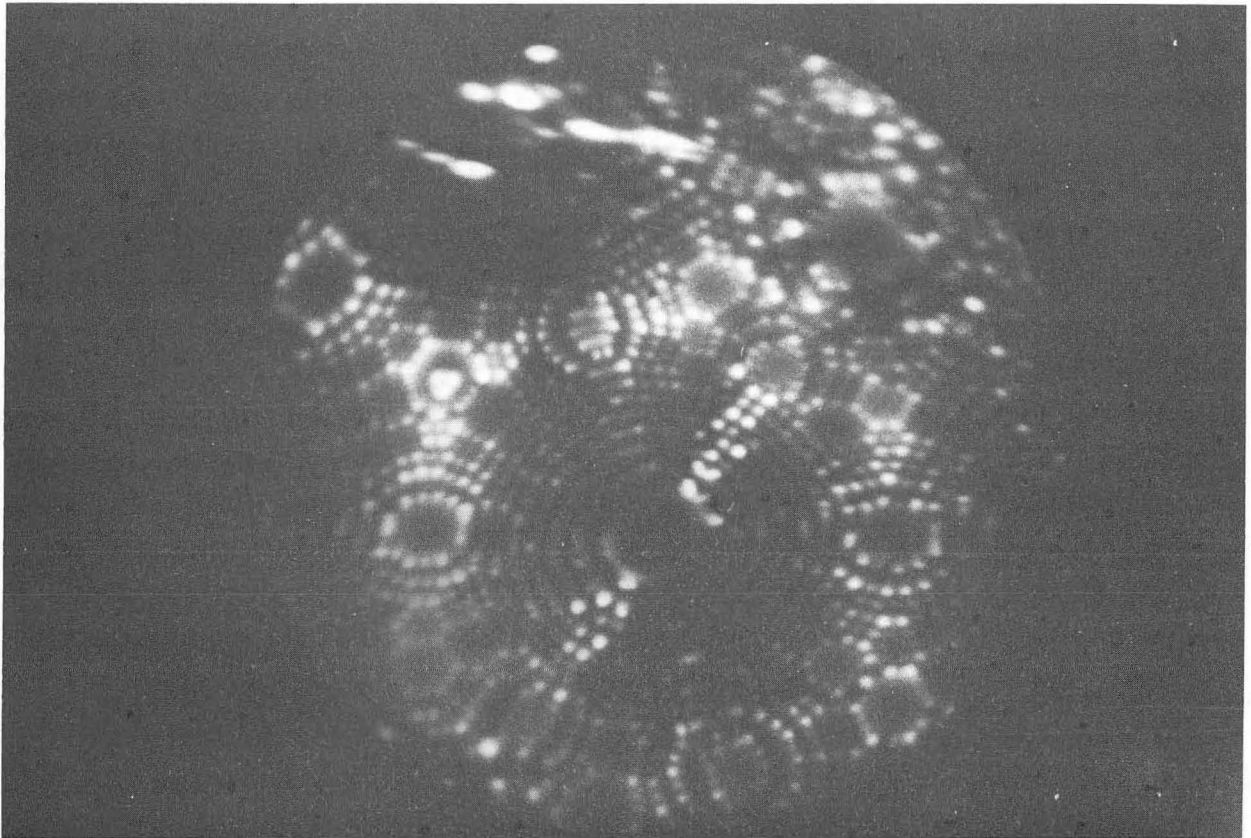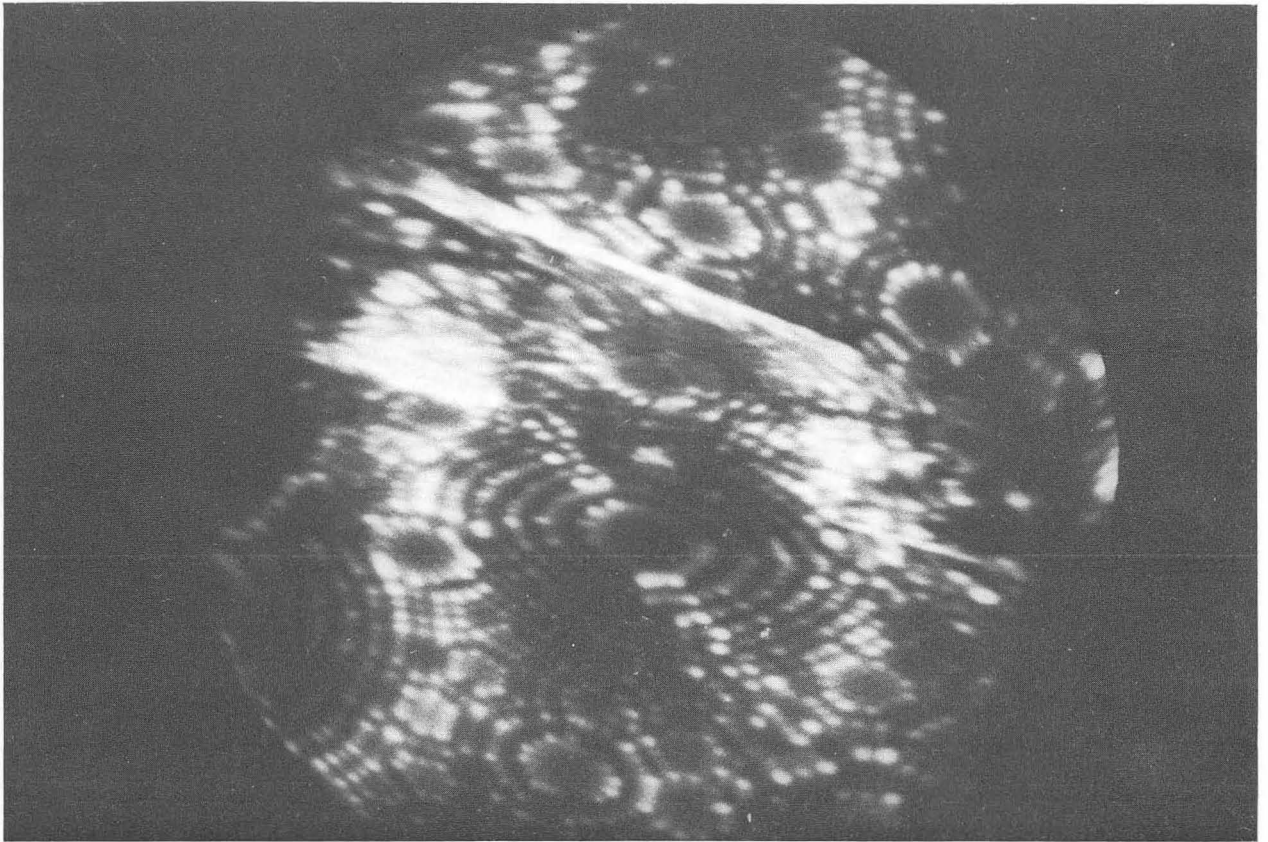
ZN-5450

Fig. 3
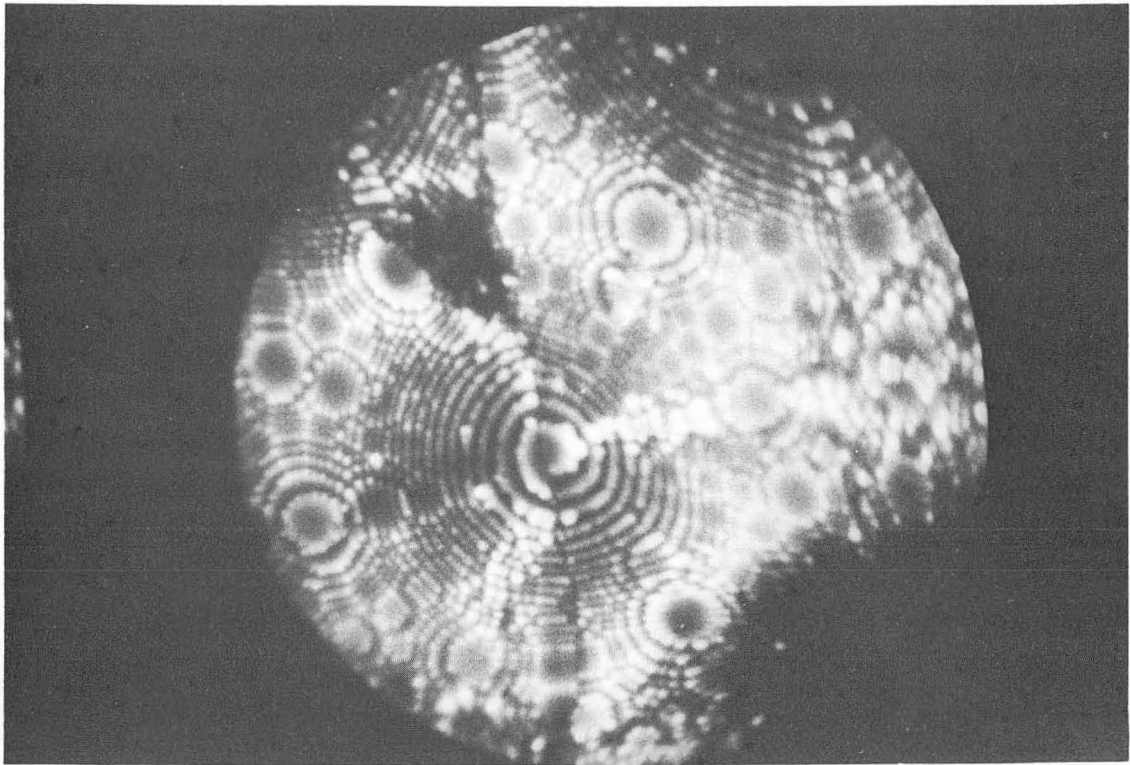
ZN-5290

Fig. 4
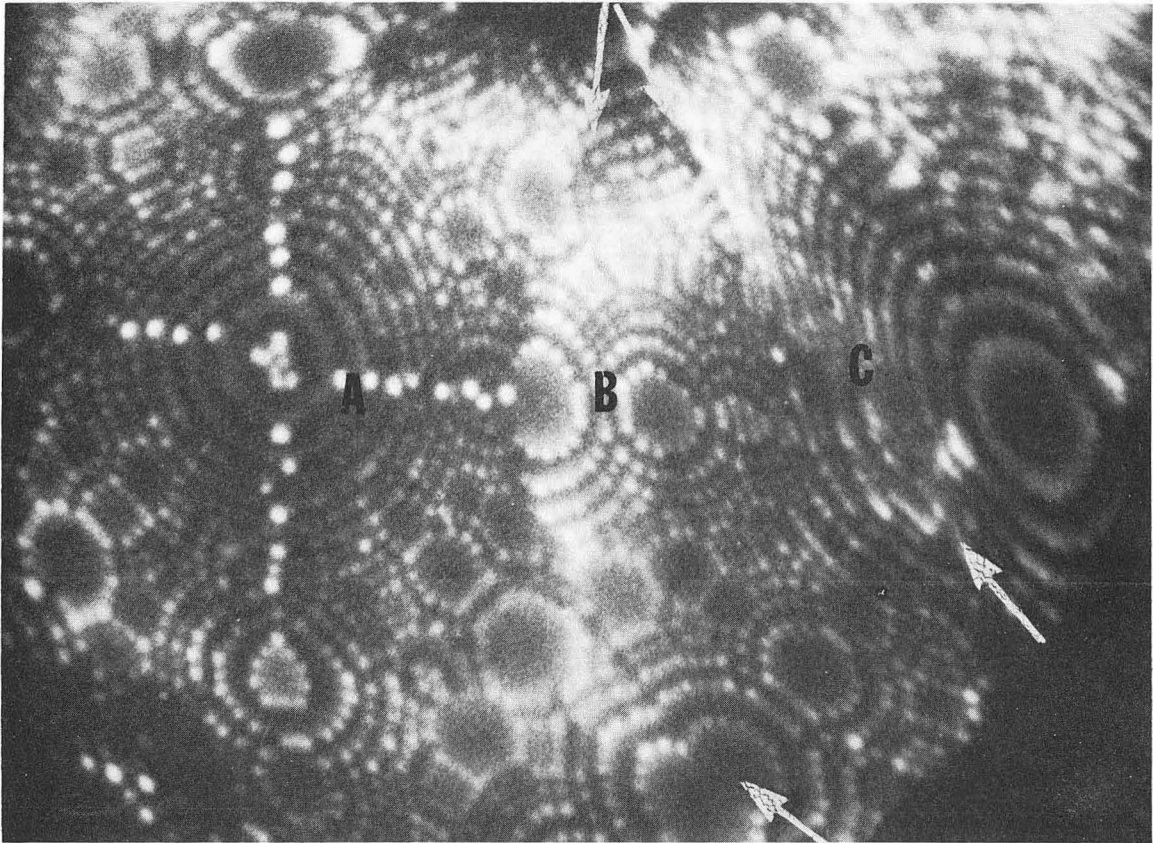
XBH671 20

Fig. 5
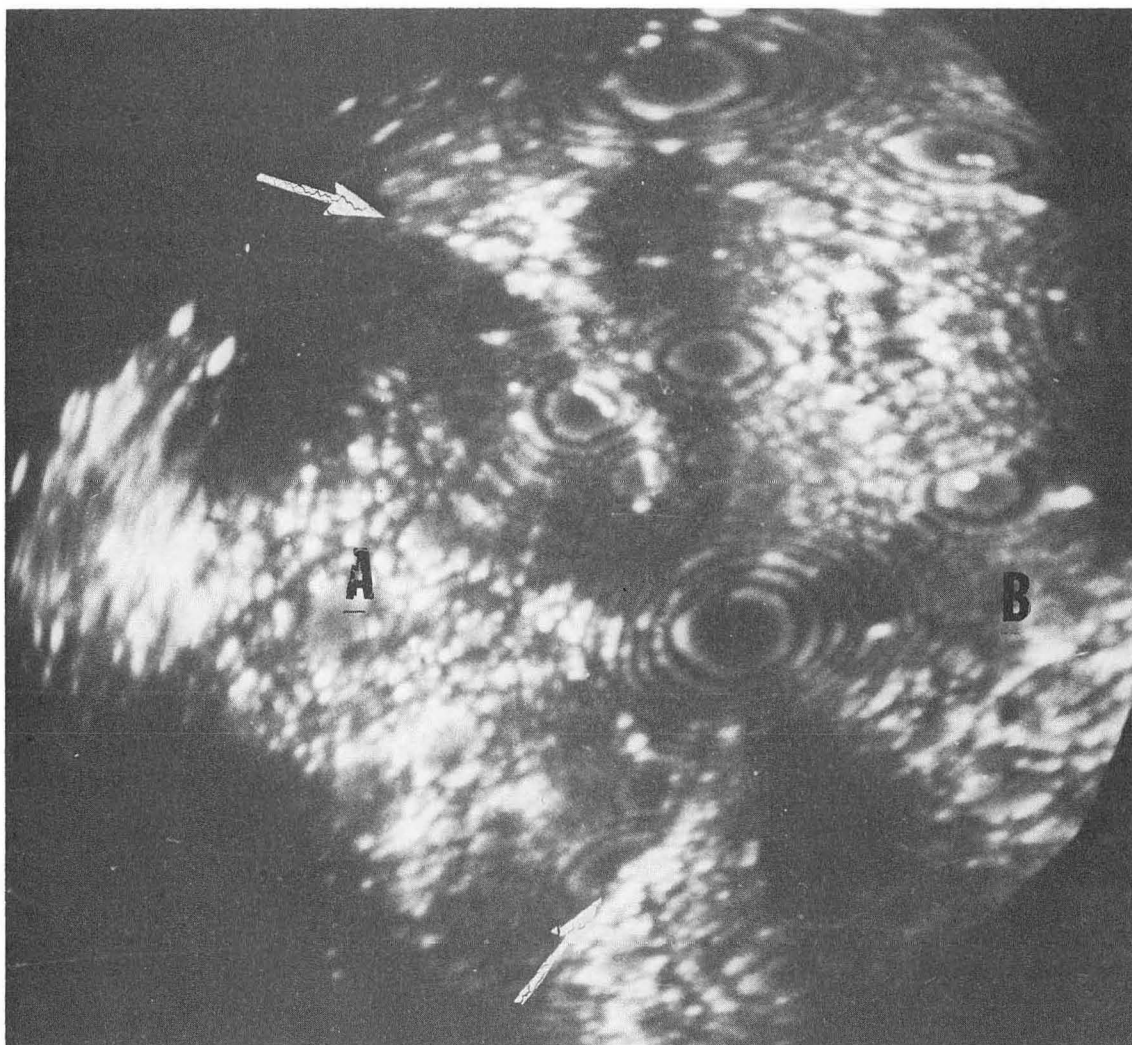
XBH671 21

Fig. 6
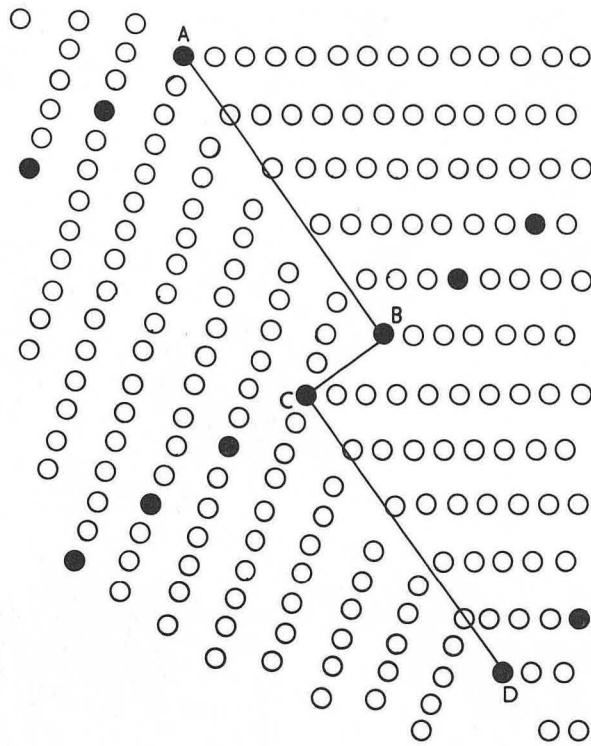
MUB-10097

Fig. 7

ZN-5458

Fig. 8